Effects of dilution on methane entering an SOFC anode

K. Kendall[*], C.M. Finnerty, G. Saunders, J.T. Chung

School of Chemical Engineering, University of Birmingham, Edgbaston, Birmingham B15 2TT, UK

Abstract

Methane and other hydrocarbons such as propane and butane are ideal fuels for SOFCs operating in portable devices for domestic or leisure use [J. Power Sources 71 (1998) 268]. This paper addresses the fuel entry conditions necessary for such devices. A gas manifold system was connected to a micro-tubular zirconia cell 2 mm diameter with lanthanum strontium manganite cathode and nickel/zirconia/ceria anode. Wire current collectors were used to obtain electrochemical performance data via a potentiostat system. The reaction products from the anode were analysed by mass spectroscopy to elucidate the reaction mechanism, and temperature programmed oxidation allowed the carbon deposition to be evaluated [Proceedings of the 4th European Solid Oxide Fuel Cell Forum, Luzern, July 2001, p.151]. Carbon deposition was substantial near open circuit voltage, when little oxygen was flowing to the anode. Dilution with inert gas or with CO_2 caused a significant change in the reaction mechanism. The conclusion was that diluted methane could be fed directly into the SOFC, and that particular compositions (e.g. biogas at 30% methane and 70% carbon dioxide) gave optimum performance with little carbon fouling. © 2002 Published by Elsevier Science B.V.

*Keywords:* Microtubular SOFC; Hydrocarbon fuels; Methane; Biogas

1. Introduction

A key question for SOFCs is what happens when hydrocarbon fuel is fed directly into an operating cell. Certain fuels, such as methanol or methanoic acid, can react cleanly to give hydrogen and carbon monoxide which generate power without fouling the SOFC [1–3]. Other fuels such as methane or butane deposit carbon which blocks the cell after a short time. Of particular interest is biogas, a natural mixture of methane and carbon dioxide, which can run in SOFCs for long periods without carbon [4,5].

The purpose of this paper is to describe experiments where methane was fed directly into a microtubular zirconia fuel cell operating under various conditions. The reactions were analysed electrochemically by observing the Nernst voltage and the change in voltage with temperature. Also, the carbon deposited on the anode of the cell was investigated by temperature programmed oxidation, using a mass spectrometer to detect oxidation products from the carbon layers.

2. Theory

The theoretical objective was to understand the various reactions of hydrocarbons such as methane directly entering

an SOFC reactor. The two most simple reactions are full oxidation (FOx) and partial oxidation (POx) shown in Reactions 1 and 2 below.

$$FOx: \quad CH_4 + 2O_2 \rightarrow CO_2 + 2H_2O \tag{1}$$

$$POx: \quad CH_4 + \tfrac{1}{2}O_2 \rightarrow CO + 2H_2 \tag{2}$$
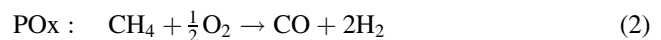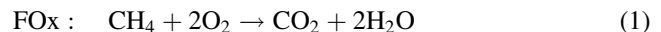
These reactions can both occur under the normal operating conditions within an SOFC. The question is, 'how can they be readily distinguished?'. Fig. 1 gives the theoretical open circuit voltage calculated from the Nernst equation, shows that the two reactions are quite distinct electrochemically. The partial oxidation gives both a higher voltage and a higher gradient with temperature than the full oxidation. Thus, by measuring the voltage and the change in voltage with temperature, the reaction can be deduced. By contrast, the reaction of pure hydrogen shown in Reaction 3, which is generally used to reduce the anode and to give a base-line performance, gives a lower voltage and a negative slope with temperature, also shown in Fig. 1. The same is true of carbon monoxide oxidation, depicted in Reaction 4 below, difficult to distinguish from hydrogen oxidation because of the similar electrochemical behaviour.

$$HOx: \quad H_2 + \tfrac{1}{2}O_2 \rightarrow H_2O \tag{3}$$

$$COOx: \quad CO + \tfrac{1}{2}O_2 \rightarrow CO_2 \tag{4}$$
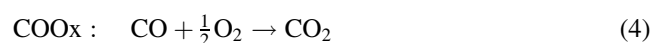
Once carbon dioxide and steam have been produced, then further reactions can occur to reform the methane on the

* Corresponding author. Tel.: +44-121-414-2739; fax: +44-121-414-5377.
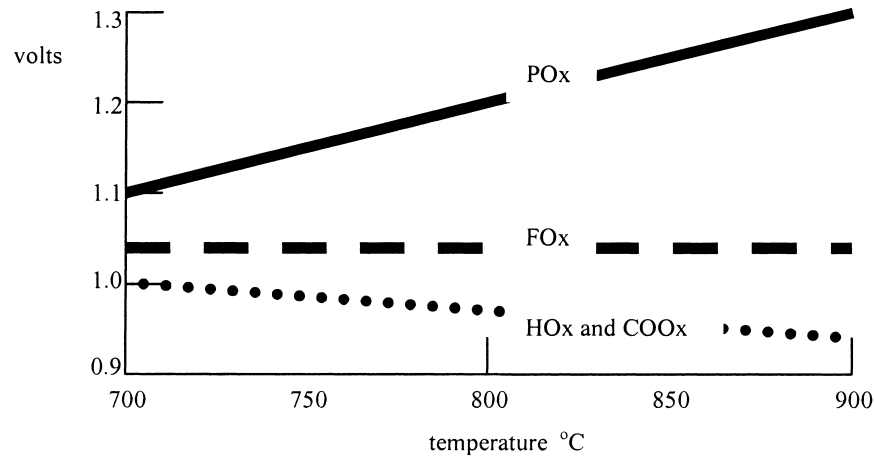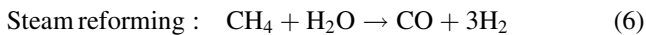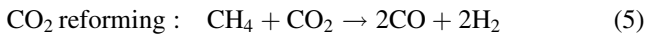*E-mail address:* k.kendall@bham.ac.uk (K. Kendall).

Fig. 1. Theoretical OCV for methane, hydrogen and CO oxidation as a function of temperature.

nickel anode. These are shown in Reactions 5 and 6, and are not detectable electrochemically in the SOFC because no oxidation reaction takes place. However, they can be detected by observing a change from methane oxidation to CO and hydrogen oxidation using the Nernst voltages, or alternatively by measuring the reaction products using a mass spectrometer.

$$CO_2 \, reforming: \quad CH_4 + CO_2 \rightarrow 2CO + 2H_2 \qquad (5)$$

$$Steam \, reforming: \quad CH_4 + H_2O \rightarrow CO + 3H_2 \qquad (6)$$

Two other reactions which can also occur to deposit carbon on the anode are methane pyrolysis and the Boudouard reaction as shown in Reactions 7 and 8. These cannot be detected electrochemically but can be inferred from temperature programmed oxidation experiments carried out to detect deposits of carbon after the fuel cell test.

$$Pyrolysis: \quad CH_4 \rightarrow C + 2H_2 \qquad (7)$$

$$Boudouard: \quad 2CO \rightarrow C + CO_2 \qquad (8)$$
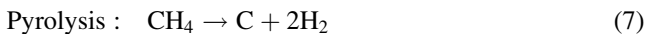
The conclusion from this theoretical argument is that certain reactions can be detected electrochemically because the voltage and voltage change with temperature are sufficiently diverse to differentiate partial oxidation and full oxidation of methane. The oxidations of hydrogen and carbon monoxide cannot be separated easily, but are distinct from the methane reactions. Thus, measurements of fuel cell voltage can be used to give significant information about hydrocarbon reactions.

3. Apparatus

The equipment used to study the fuel reaction in the SOFC is shown in Fig. 2. Electrical heating was used to warm-up the furnace to the operating temperature, between 700 and 900 °C. The fuel cell tube is shown passing through the
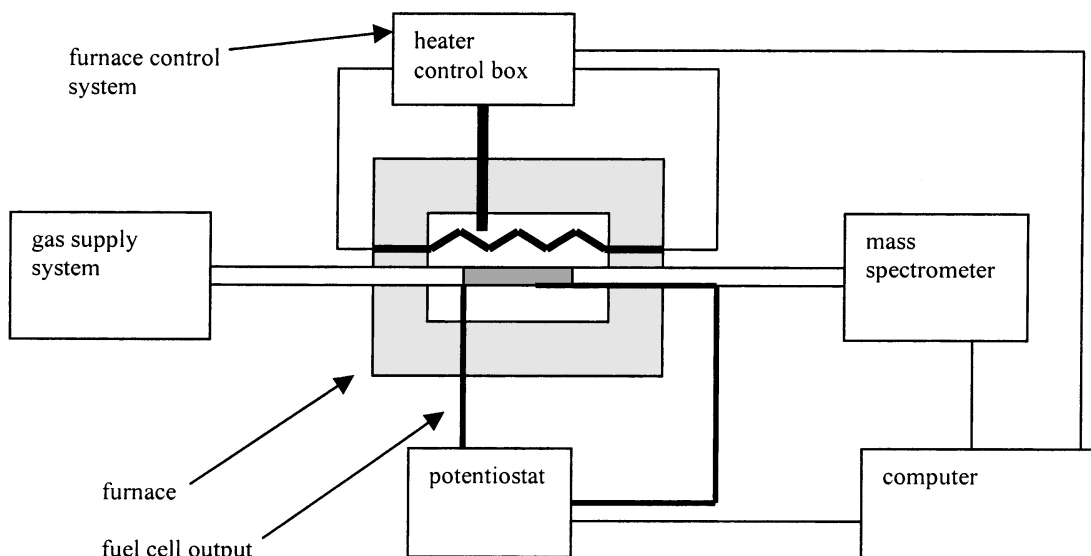

Fig. 2. System used to study micro-tubular SOFCs.

furnace box, connected to a gas supply system at the entry and to a mass spectrometer at the exit. Each cell tube was made by extruding cubic zirconia paste from a 2.5 mm diameter die to give a wall thickness of 200 μm. The tube was fired at 1500 °C to make it fully dense, then coated on the inside with nickel cermet anode containing 5% cerium oxide, firing again to 1300 °C. Outside, a two layer cathode coating of lanthanum–strontium manganite was deposited, fired to 1100 °C. A nickel current collector wire was inserted down the tube to make contact with the anode layer, and a silver wire was wrapped around the cathode. A potentiostat was used to measure the voltage across the cell and to draw current. Each cell anode was reduced in hydrogen at 800 °C.

Fuel gas was supplied to the tubular cell using a flow controller from a plastic bag which was filled with the desired gas mixture from cylinders. The products of reaction were sampled by a mass spectrometer during a fuel cell run. After the run, the carbon deposited was analysed by temperature programmed oxidation of the anode. A computer controlled the experiments and logged the data.

4. Experimental results

In the first experiment, the open circuit voltages were measured for both hydrogen and methane to check the Nernst theoretical argument (Fig. 3). The gases were passed through the cell at 2–8 ml/min and the voltages were measured. In the case of hydrogen, it was clear that steam addition was necessary to obtain the equilibrium condition, so this was provided in a humidifier operating at 74 °C, to give a concentration of 30% steam in the gas mixture. The results fitted the theory very well and showed that both the Nernst voltage and its gradient with temperature could be used to assess the reaction conditions.

In the methane experiment, there was no doubt that carbon was depositing on the anode, because the electrodes became blocked after 30 min of operation. This indicated that pyrolysis and/or Boudouard reactions were occurring in addition to simple partial oxidation. Temperature programmed

oxidation experiments also proved that carbon was forming in a short time after exposing the anode to methane.

The next test was to mix the methane with helium to investigate the influence of inert diluent on the anode reaction mechanism. Methane–helium mixtures were prepared in a plastic bag, then passed at 2 ml/min down the fuel cell tube at several temperatures. The results are shown in Fig. 4 to show the strong effect of dilution on the reaction mechanism. At 100% methane the voltage is almost that given by the Nernst equation for partial oxidation, with a steep gradient as temperature increased. However, when more than 75% of helium was added to the methane the situation changed above 800 °C. Then the gradient was negative with temperature, indicating full oxidation or reaction of hydrogen or CO with oxygen. Fig. 4 shows the results for a mixture of 10% methane and 90% helium. It was evident from TPO experiments that only a small amount of carbon was depositing on the anode under these conditions. The conclusion was that dilution was causing a significant change in the reaction mechanism, from partial oxidation with disastrous carbon deposition to complete oxidation with minimal carbon.

An even more striking picture was obtained when carbon dioxide was used as the additive gas, as shown in the lower results of Fig. 4. These results now almost fitted the full oxidation theory curve, but with a slight negative slope which could indicate hydrogen or CO oxidation. TPO measurements indicated little carbon on the anode under this condition. Levels of carbon dioxide below 60% gave partial oxidation behaviour and carbon deposits. The conclusion was that addition of carbon dioxide was a most effective method for preventing partial oxidation of methane leading to carbon deposition.

A possible explanation for this effect is the blocking of the nickel surface sites by the diluent gas molecules. Whereas concentrated methane is adsorbed at many adjacent sites on nickel to produce carbon layers, the diluent molecules interfere with this process by co-adsorbing and separating the carbon atoms, allowing oxygen to diffuse from the zirconia/nickel boundary to give full oxidation. In the case
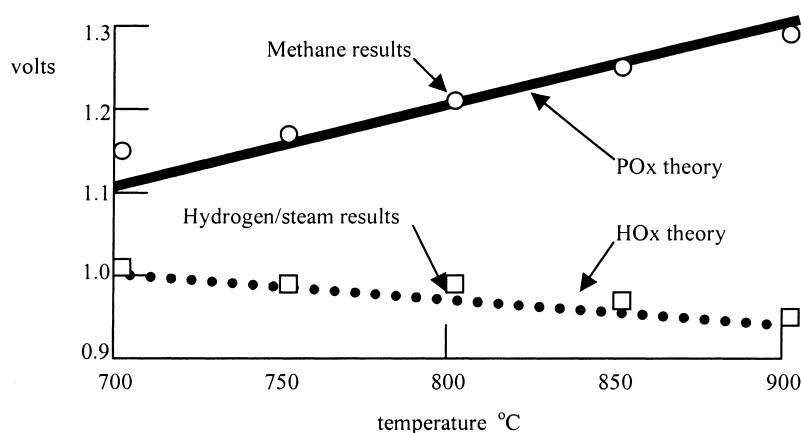

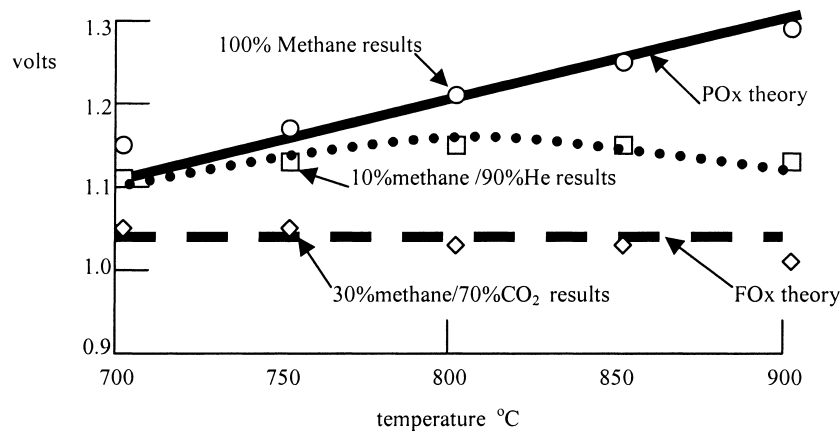Fig. 3. Comparison of Nernst theory and results for methane and hydrogen/steam.

Fig. 4. Change in anode potential on dilution with helium.

of CO_2 at high concentrations, the carbon can also react with the adjacent carbon dioxide molecules on the nickel surface, thereby preventing bulk carbon deposition.

5. Significance for SOFC application

The significance of this result is that it suggests that pure methane is an inferior fuel for SOFCs compared with biogas at 60% methane and 40% carbon dioxide. Biogas of this composition can still give an open circuit voltage near 1 V and power output comparable with pure methane. These results are shown in Figs. 5 and 6.

Fig. 5 was obtained by plotting the open circuit voltage results for the SOFC as a function of methane concentration on a logarithmic scale. As the methane was diluted with helium, the voltage at 900 °C dropped-off nearly according to the Nernst equation, falling from 1.3 V for pure methane to about 1.1 V with 5% methane. The result at 20% methane was lower than expected from partial oxidation, suggesting that a change in reaction mechanism had occurred at this

high dilution. With carbon dioxide, the fall-off in voltage was much more rapid, reaching 1 V for 20% methane at 800 °C.

These ideas were borne out by power output results at different methane concentrations in carbon dioxide, plotted in Fig. 6 for flow of 4 ml/min at 850 °C. Two curves are given, one for maximum power output at 0.5 V and the other in cruise mode at 0.7 V. Concentrated methane gave reduced power output because of carbon deposition, and this dropped rapidly with time because the cell became totally blocked with carbon after about 30 min. By contrast, at 30–40% methane in carbon dioxide, the power output was the same as for pure methane, but now the cell remained cleaner and carbon deposition was much reduced. At lower methane levels, the power output decreased steadily to nought at zero methane, along an almost parabolic curve. Such a power output curve is in marked contrast to that from an internal combustion engine where ignition problems become severe below 50% methane. A schematic curve for a spark ignition diesel engine is shown with a relatively low efficiency and a cut-off in power at 50% methane. These results show clearly
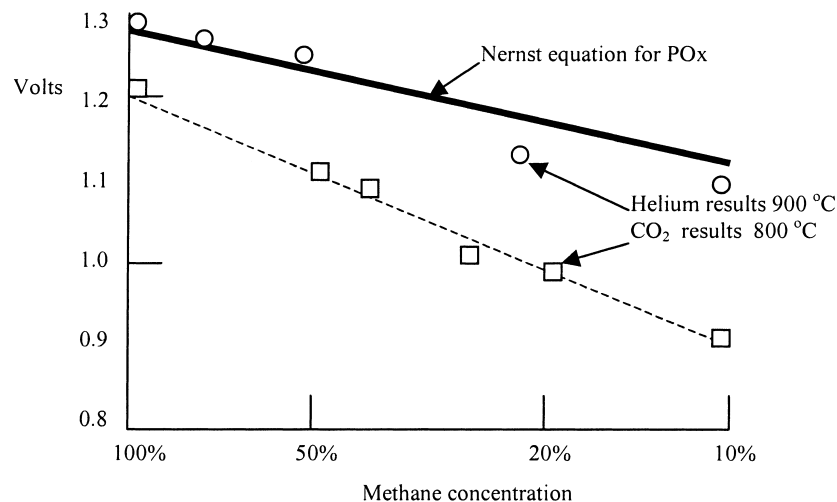
Fig. 5. Fall in open circuit voltage when methane was diluted with helium or carbon dioxide.
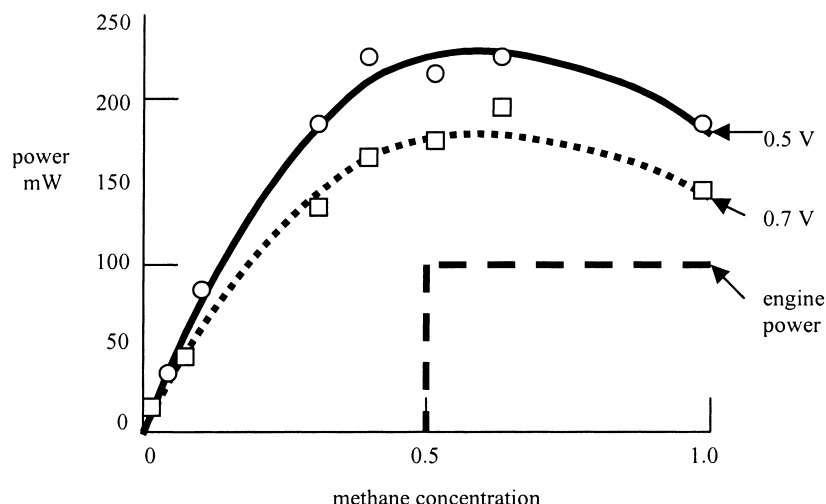
Fig. 6. Power output of fuel cell running on methane/CO_2 mixtures.

that a fuel cell can operate efficiently on a depleted biogas composition around 30% methane, whereas an internal combustion engine fails at this condition.

6. Conclusions

Mixtures of methane and gases such as helium or carbon dioxide have been tested in small tubular SOFCs, then analysed by observing the open circuit voltage, the change of this voltage with temperature and the carbon deposition using mass spectroscopy. Pure methane gave open circuit voltage results consistent with partial oxidation of methane. There was much carbon deposition which blocked the 2 mm diameter tubes in about 30 min. Diluting with helium reduced the OCV as expected from the Nernst equation but it was seen that at 10% methane, full oxidation seemed to occur as evidenced by the lowering of OCV with increasing

temperature. Dilution with CO_2 gave a logarithmic lowering of OCV but steeper than that for helium. A mixture of 30% methane with 70% carbon dioxide seemed to fit the full oxidation curve. Power output at this composition was good and there was little carbon fouling [6]. SOFCs are superior to IC engines for such fuel compositions.

References

[1] K. Kendall, M. Palin, J. Power Sources 71 (1998) 268–270.
[2] C M.. Finnerty, T Alston, R.M. Ormerod, K. Kendall, in: A.J. McEvoy (Ed.), proceedings of the 4th European Solid Oxide Fuel Cell Forum, Luzern, July 2000, pp. 151–158.
[3] G. Saunders, K. Kendall, J. Power Sources, this volume.
[4] J. Staniforth, K. Kendall, J. Power Sources 71 (1998) 275–777.
[5] J. Staniforth, K. Kendall, J. Power Sources 86 (2000) 401–403.
[6] G. Saunders, K. Kendall, Patent Application No. GB 0020478.4 (2000).